Problem 1

A two-dimensional cavity is filled with an incompressible Newtonian fluid. The fluid is driven by the lid moving with a constant velocity U. The cavity has dimensions $H \times H$. Find the steady state solution.

(a) **Describe the essential steps for the Lattice Boltzmann Method.**

0.1 D2Q9 Lattice

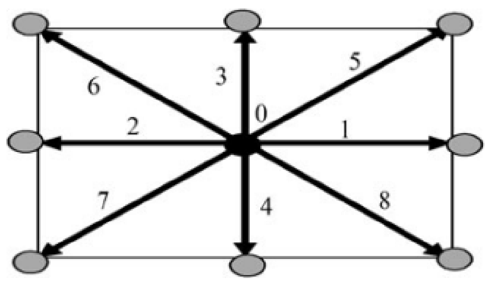

Figure 1: D2Q9 Lattice arrangement (Mohamad p.21).

0.2 Lattice Boltzmann Method

The method consists of two steps, collisions and streaming. The collision step without a forcing function is:

$$f_k(x, y, t + \Delta t) = f_k(x, y, t)[1 - \omega] + \omega f_k^{eq}(x, y, t) \tag{1}$$

where $k = 0, ..., 8$. The streaming step is:

$$f_k(x + \Delta x, y + \Delta y, t + \Delta t) = f_k(x, y, t + \Delta t) \tag{2}$$

where $k = 0, ..., 8$. In the streaming process, we have the following:

$f_1(i, j) \rightarrow f_1(i + 1, j)$
$f_2(i, j) \rightarrow f_2(i, j + 1)$
$f_3(i, j) \rightarrow f_3(i - 1, j)$
$f_4(i, j) \rightarrow f_4(i, j - 1)$
$f_5(i, j) \rightarrow f_5(i + 1, j + 1)$
$f_6(i, j) \rightarrow f_6(i - 1, j + 1)$
$f_7(i, j) \rightarrow f_7(i - 1, j - 1)$
$f_8(i, j) \rightarrow f_8(i + 1, j - 1)$

The movement of these points correspond to the values of the streaming velocity along the lines: $c_0(0,0), c_1(c,0), c_2(0,c), c_3(-c,0), c_4(0,-c), c_5(c,c), c_6(-c,c), c_7(-c,-c), c_8(c,-c)$ where $c = \Delta x/\Delta t$. The values of the weighting factors are:

$w(0) = 4/9$
$w(1) = w(2) = w(3) = w(4) = 1/9$
$w(5) = w(6) = w(7) = w(8) = 1/36$

0.3 BGK Collision Operator

The lattice Boltzmann is written in equation (1). The equilibrium distribution function is defined by:

$$f_k^{eq} = w_k \rho(x,t)\left[1 + \frac{c_k \cdot \mathbf{u}}{c_s^2} + \frac{1}{2}\frac{(c_k \cdot \mathbf{u})^2}{c_s^4} - \frac{1}{2}\frac{\mathbf{u}^2}{c_s^2}\right] \tag{3}$$

where

$$c_s = \frac{c_k}{\sqrt{3}} \tag{4}$$

$$c_k = \frac{\Delta x}{\Delta t}\hat{i} + \frac{\Delta y}{\Delta t}\hat{j} \tag{5}$$

$$\mathbf{u} = u\hat{i} + v\hat{j} \tag{6}$$

Since c_k are unit vectors, we can use:

$$f_k^{eq} = w_k \rho(x,t)\left[1 + 3(c_k \cdot \mathbf{u}) + \frac{9}{2}(c_k \cdot \mathbf{u})^2 - \frac{3}{2}\mathbf{u}^2\right] \tag{7}$$

0.4 Mach and Reynolds Numbers

The fluid viscosity is related to the relaxation frequency as:

$$\nu = \frac{\Delta x^2}{3\Delta t}(\omega - 0.5) \tag{8}$$

Dividing both sides of the equation by UL, this yields the mach number:

$$Ma = \frac{\Delta x}{L\sqrt{3}}(\omega - 0.5)Re \tag{9}$$

The Mach number should be low for incompressible flow simulation using the Lattice Boltzmann Mathod (LBM). As a normal practice in LBM, Δx is unity such that $L = N$. Hence, $Re = UN/\nu$ is the lattice Reynolds number. For an accurate solution, the Mach number should be kept small by choice of ω or N. In general, U should be in the order of 0.1 or 0.2. The macroscopic Reynolds number should equal the LBM Reynolds number such that U and ν can be arbitrarily selected within the range that insures the stability of the solution. Care should be taken in using very small values of ν which may cause a stability issue.

0.5 Mass and Momentum Conservation

The summation of distribution functions at each lattice site represents the macroscopic fluid density:

$$\rho = \sum_{k=0}^{8} f_k \tag{10}$$

The momentum can be represented as an average of the lattice velocities c_k weighted by the distribution function:

$$\mathbf{u} = \frac{1}{\rho} \sum_{k=0}^{8} f_k \mathbf{c_k} \tag{11}$$

0.6 Boundary Conditions

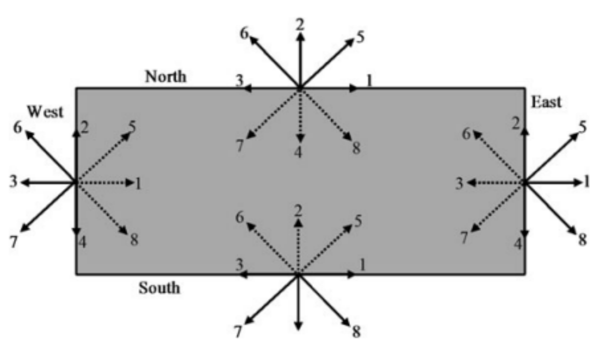

Figure 2: Distribution functions at the boundaries of a domain (Mohamad p.76).

Bounce back on the West boundary:

$f_1 = f_3$
$f_5 = f_7$
$f_8 = f_6$

Bounce back on the South boundary:

$f_2 = f_4$
$f_5 = f_7$
$f_6 = f_8$

Bounce back on the East boundary:

$f_3 = f_1$
$f_6 = f_8$
$f_7 = f_5$

Bounce with known velocity on the North boundary:

$$\rho_N = [f_0 + f_1 + f_3 + 2(f_2 + f_6 + f_5)] \tag{12}$$

$$f_4 = f_2 \tag{13}$$

$$f_7 = f_5 - \frac{1}{6}\rho_N u_N \tag{14}$$

$$f_8 = f_6 + \frac{1}{6}\rho_N u_N \tag{15}$$

Where $u_N = U$ is the lid velocity, $v_N = 0$ and $f_3 = f_1$.

0.7 Algorithm

Define the lid velocity U, initial liquid density ρ, number of grid points N, viscosity ν, spacing $\Delta x = \Delta y = 1$ and time interval $\Delta t = 1$.

Compute the Reynolds number $Re = UN/\nu$ and the relaxation frequency ω (Eq.9). Initialize the grids for u-velocity, v-velocity, and density by having equal density everywhere and velocities zero everywhere except $u = U$ at the north boundary. Initialize the weights $w(k)$ and the streaming velocities c_k as described in Section 0.2.

Iterate these steps:

- Update f_k and f_k^{eq} using the collision step (Eq.1) with the equilibrium function (Eq.8).

- Execute the streaming step to update f_k (Eq.2).
- Implement the boundary conditions for f_k as defined in Section 0.6.
- Update the density ρ and the interior velocities u, v using equations 10 and 11. Use equation 12 for density at the North boundary.

0.8 Simulation Criteria

The initial conditions of the simulation are as follows:

Velocity u: $U = 0.4$ at the lid, zero elsewhere
Velocity v: zero everywhere
Density ρ: 1 everywhere
Domain H = 1
N = 128 grid points in either direction
Dynamic viscosity: $\nu = UN/Re$
$\tau = (3\nu + 0.5)$
$\omega = 1/\tau$
$h = \Delta x = \Delta y = 1$
Mach number: $Ma = Re(\omega - 0.5)/(N\sqrt{3})$
$\Delta t = 1$
Max time steps = 40000
Max error = 1e-6

The error at each time step is $max(du + dv)$ where $du = u^{t+1} - u^t$ and $dv = v^{t+1} - v^t$. This quantifies how much the values of u, v change between iterations. The loop can end if it hits the maximum number of time steps or the solution converges within the maximum error 10×10^{-6}.

(b) **Compute the steady state solutions for $\boldsymbol{Re} = 100$, $\boldsymbol{Re} = 400$, and $\boldsymbol{Re} = 1000$.**

0.9 Comparison to Literature

Resource: Ghia, U. K. N. G., Kirti N. Ghia, and C. T. Shin. "High-Re solutions for incompressible flow using the Navier-Stokes equations and a multigrid method." *Journal of computational physics* 48.3 (1982): 387-411.

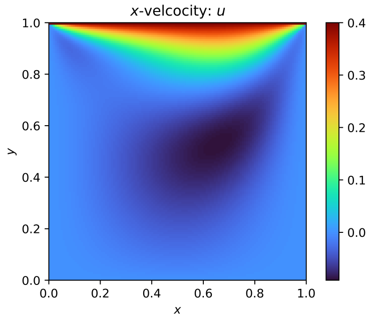

(a) Velocity u.

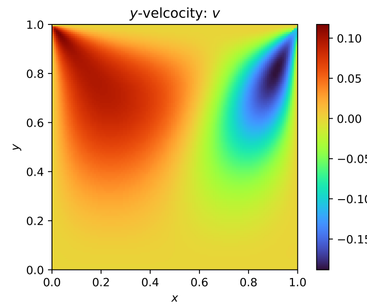

(b) Velocity v.

Figure 3: Steady state u, v grids at *Re = 100*.

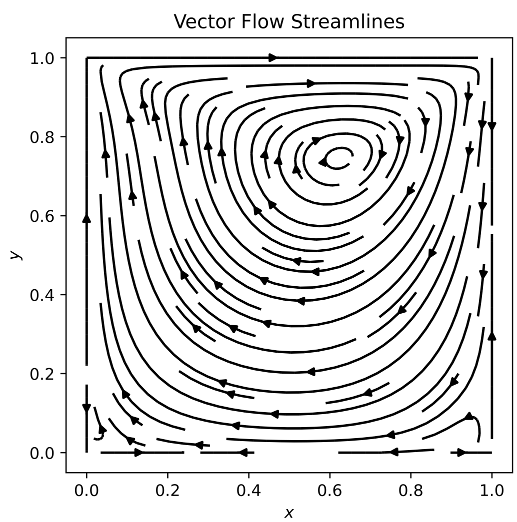

Figure 4: Steady state streamlines at *Re = 100*.

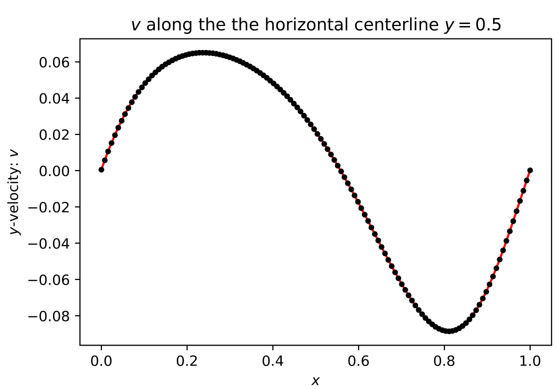

(a) Velocity u at horizontal centerline.

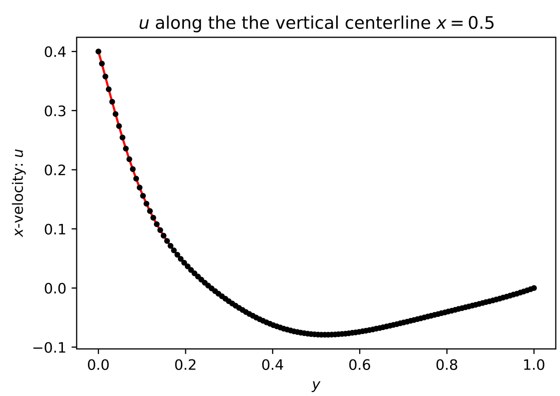

(b) Velocity v at vertical centerline.

Figure 5: Steady state u and v at *Re = 100*.

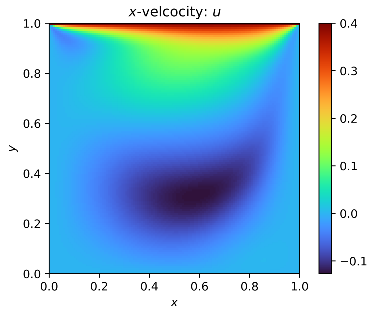

(a) Velocity u.

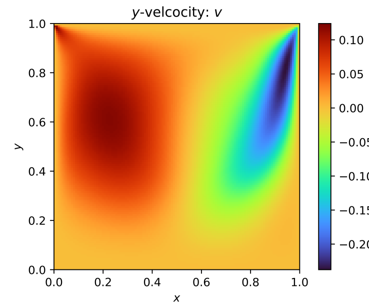

(b) Velocity v.

Figure 6: Steady state u, v grids at Re = *400*.

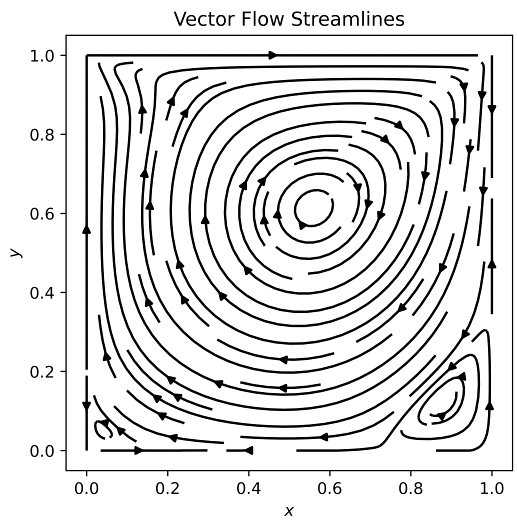

Figure 7: Steady state streamlines at Re = *400*.

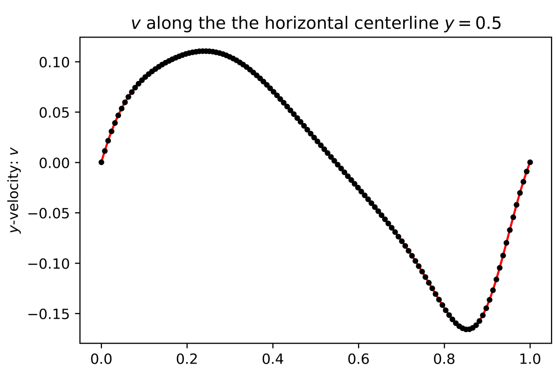

(a) Velocity u at horizontal centerline.

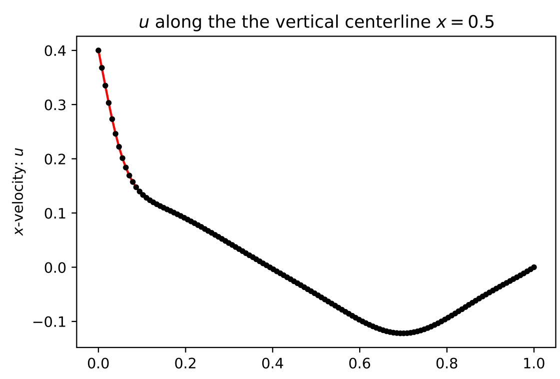

(b) Velocity v at vertical centerline.

Figure 8: Steady state u and v at Re = *400*.

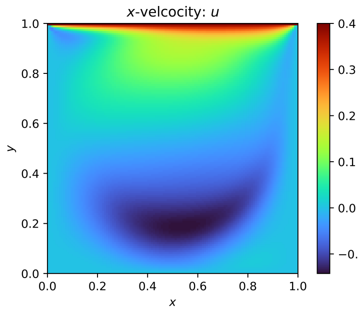

(a) Velocity u.

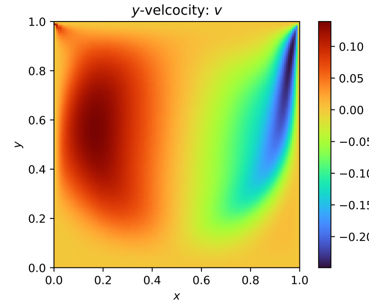

(b) Velocity v.

Figure 9: Steady state u, v grids at *Re = 1000*.

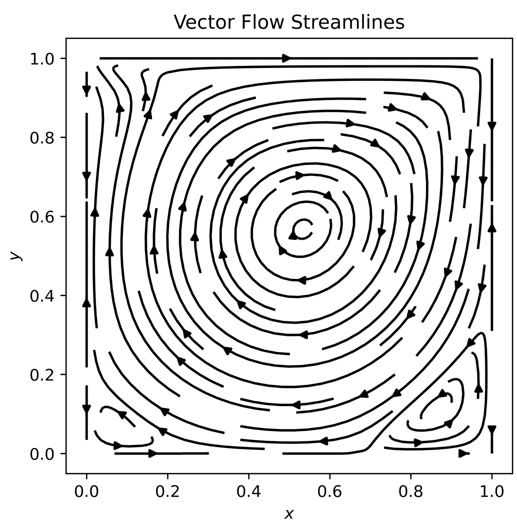

Figure 10: Steady state streamlines at *Re = 1000*.

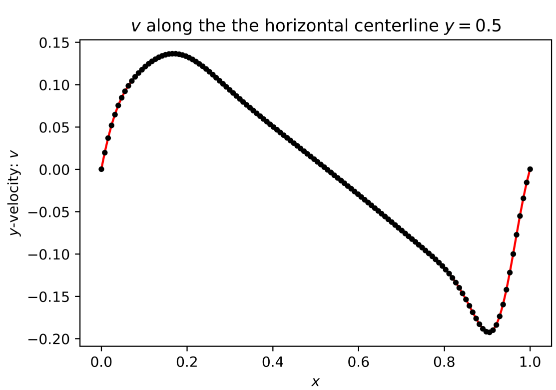

(a) Velocity u at horizontal centerline.

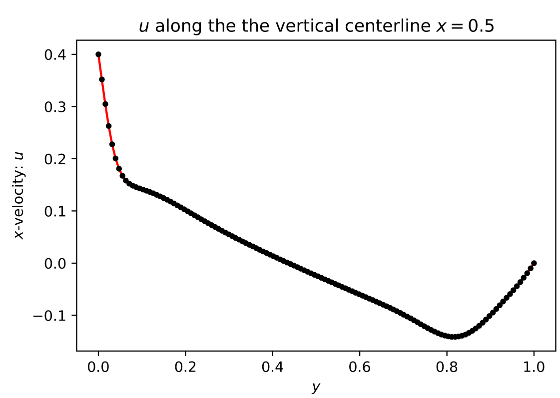

(b) Velocity v at vertical centerline.

Figure 11: Steady state u and v at *Re = 1000*.

The steady state streamlines for $Re = 100$ (Fig.4) and $Re = 400$ (Fig.7) look similar to those in the resource. From $Re = 100$ to $Re = 400$, the main vortex shifts downward and the vortices in the bottom corners of the cavity become larger. Increasing the Reynolds number to $Re = 1000$, the main vortex shifts more toward the cavity center and the vortices in the bottom corners become even more prominent as we would expect (Fig.10).

We define the minimum velocity at the vertical centerline as u_{min}, the minimum velocity at the horizontal centerline as v_{max}, and the maximum velocity at the horizontal centerline as v_{max} (See Figures 4 and 7). These values are compared to the literature values in Table 1, where percent error is defined as:

$$\delta = \frac{|simulation\text{ - }resource|}{|resource|} \times 100\% \tag{16}$$

It is important to note that the velocities in Table 1 are scaled to match the lid velocity $U = 1$. Since the simulations were executed with $U = 0.4$, the velocities were simply multiplied by 2.5. Simulation constants are displayed in Table 2. The choice of a large grid for comparison to literature was used to minimize the Mach number at $Re = 1000$. The choice of $U = 0.4$ was selected to minimize the Mach number but not have instability with too small ν or with too large U.

Velocity	Re	Simulation	Resource	% Error
u_{min}	100	-0.19760	-0.21090	6.3%
v_{min}	100	-0.22149	-0.24533	9.7%
v_{max}	100	0.16261	0.17527	7.2%
u_{min}	400	-0.30489	-0.32726	6.8%
v_{min}	400	-0.41426	-0.44993	7.9%
v_{max}	400	0.27644	0.30203	8.5%
u_{min}	1000	-0.35328	-0.38289	7.7%
v_{min}	1000	-0.48110	-0.51550	6.7%
v_{max}	1000	0.34160	0.37095	7.9%

Table 1: Comparison of simulation and resource values for u_{min}, v_{min}, and v_{max}.

The errors at each Reynolds number are all below 10%. This suggests that the program inputs may need to be tweaked to reduce the error, or that main vortex center, instead of geometric center, may be a better comparison for future assessments. Overall, the errors are still within an acceptable range and show that the program is simulating what we want, but has room for improvement.

Re	Ma	ν	τ
100	-0.00270	0.508	2.024
400	1.15	0.127	0.8810
1000	4.70	0.0508	0.6524

Table 2: Simulation constants.

(c) **For $\boldsymbol{Re} = 100$ and $\boldsymbol{Re} = 400$, qualitatively show your two velocity profiles are converging to the literature values by considering three different grid sizes with the grid resolution doubled each time.**

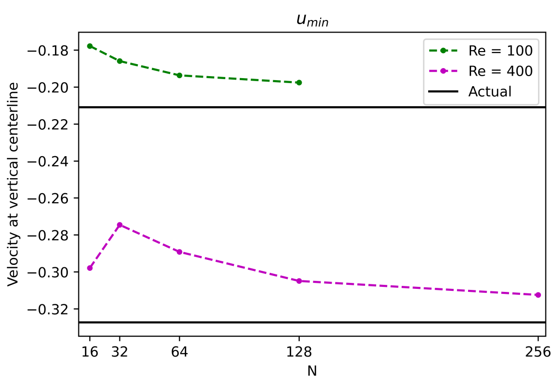

(a) u_{min}.

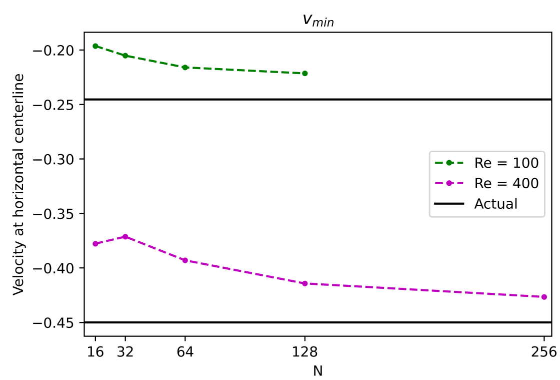

(b) u_{min}.

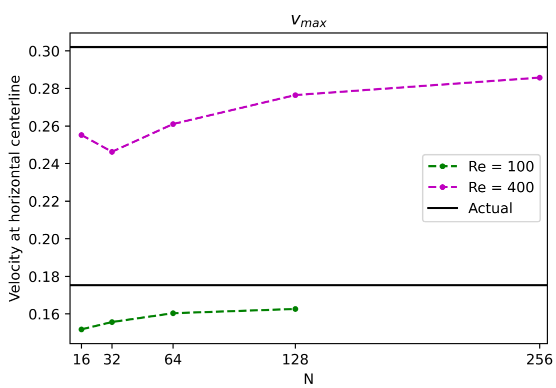

(c) v_{max}.

Figure 12: Comparison of velocities from centerline profiles.

The general trend of the plots in Fig.12 is that the minimum and maximum velocities of the centerline plots are slowly nearing the literature values as the grid size N is increased. It is notable that the higher Reynolds solutions require larger N to be as close to the literature result as for the smaller Reynolds solutions.

(d) **Numerically compute the spatial convergence rate of your scheme.**

We take the L2 norm over the sum of all differences in velocities u or v between the grids with $N = \{16, 32, 64\}$ points and the solution with 128 grid points as the spatial error measurement. Since the values at the boundaries are constant between solutions, making the differences in solutions zero along the boundary, $(N-2)^2$ points on the grid provide meaningful data and are used to compute the error.

$$\epsilon|_u = \frac{\sqrt{\sum_{i,j}(u_N - u_{128})^2_{ij}}}{(N-2)^2} \tag{17}$$

To execute this, the solution of the grid with 128 points is restricted to match the grid sizes $N = \{16, 32, 64\}$. Meaning, the results from the finer grid are interpolated to a coarser grid. A restriction function was created which implements the boundary conditions for u, v and then averages the 8 fine mesh neighbors of the coarse point (N, S, E, W, NE, NW, SE, SW) in 2D, restricting the grid to a $N/2$ mesh. The 128 point grid was first restricted to $N = 64$, then it was recycled into the function to get the restriction at $N = 32$. The function was executed once more to restrict the 128 point grid to $N = 16$. Since the execution time would have taken a day to compute the $N = 128$ grid using the projection method, I substituted the data from the artificial compressibility method.

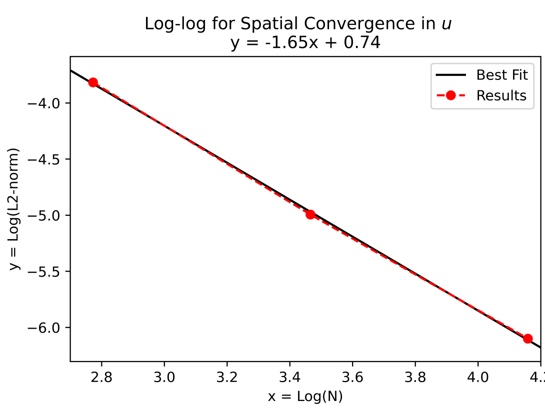

(a) Velocity u, Convergence rate = 1.65.

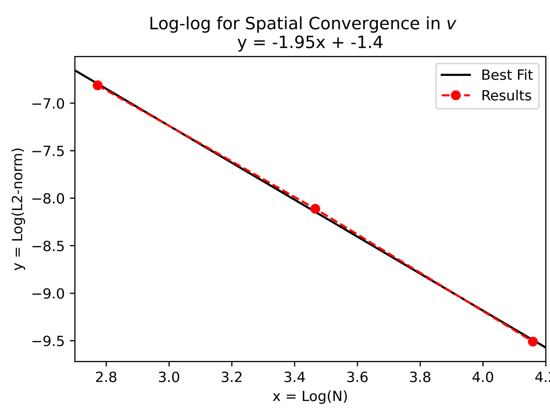

(b) Velocity v, Convergence rate = 1.95.

Figure 13: Spatial convergence in u and v at Re = *100.*

The spatial convergence rate for v is close to 2 for $Re = 100$ and $Re = 400$(Fig.8). This agrees with what we would expect for the spatial convergence rate for a second order scheme. On the other hand, the convergence rate for u is 1.65. Some authors claim bounce back boundaries are first order accurate (Mohamad p.74). Thus, there may be some justification or artifact explaining why u has a slower spatial convergence rate.

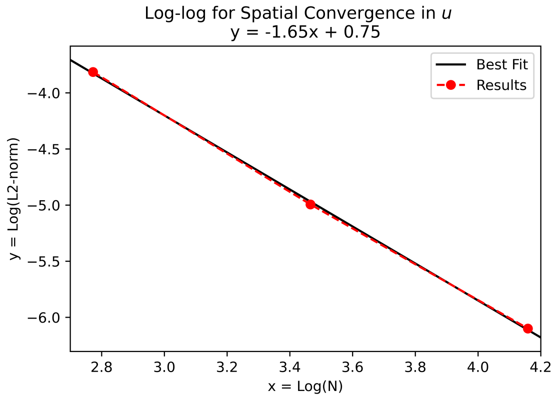

(a) Velocity u, Convergence rate = 1.65.

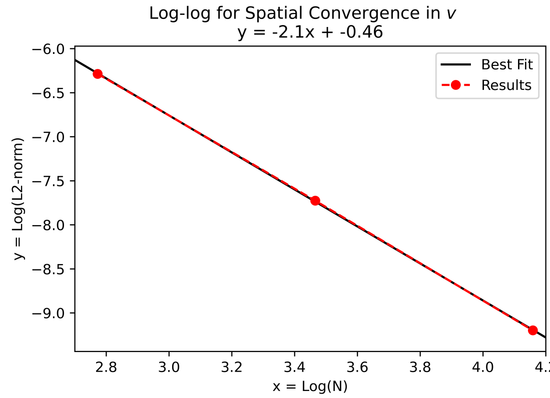

(b) Velocity v, Convergence rate = 2.1.

Figure 14: Spatial convergence in u and v at $Re = 400$.

(e) **Examine the effect of the relaxation time τ and the Mach number on method stability. Compare your results to the stability criteria. Discuss how these parameters impact the feasible range of Reynolds numbers, required grid size and physical time step size.**

As stated in Section 0.4:

$$\tau \propto \nu = \frac{UN}{Re} \tag{18}$$

$$Ma \propto \frac{1}{\tau} \tag{19}$$

We want to keep the Mach number small which means that τ will be compromised a bit even though it should be kept small as well, since, too small ν can cause instability. This impacts the range of Reynolds numbers that can be used. Since, too large $\Re$ will cause ν and τ to be quite small.

Test at Re=400 with the velocity computed from ν with grid size 41 x 41 (Table 3).

ν	U	Ma	τ	u_{min}	v_{min}	v_{max}
0.08	0.8	4.9	0.74	-0.46	-0.57	0.38
0.06	0.6	5.6	0.68	-0.39	-0.51	0.34
0.04	0.4	6.4	0.62	-0.28	-0.38	0.25
0.02	0.2	7.4	0.56	-0.15	-0.20	0.13

Table 3: Results for changing ν.

From the above table, $\nu = 0.04$ provides results closest to the literature values $u_{min} = -0.33$, $v_{min} = -0.45$, and $v_{max} = 0.30$. Values of ν above 0.08 caused the program not to run and Values 0.02 and below started to lack smoothness in the plotted solutions for u, v.

It is best for the grid size to be large because it decreases the Mach number and does not come with the instability of too large U and gives more freedom of Reynolds number choice.

It is notable that the physical time step size Δt also impacts the stability because ν is proportional to the inverse of Δt such that if the time step increases, the Mach number increases. And, if the time step decreases, the Mach number decreases.

(f) **Compare LBM to the projection method and artificial compressibility method from the previous homeworks.**

The artificial compressibility method and the projection method had similar accuracies when compared to the literature data. Overall, the artificial compressibility method was a faster running algorithm because it did not implement an integration method (Gauss/SOR). On the other hand, the LB method is much faster since it could compute the 128 x 128 solution in about a half hour. In contrast, the artificial compressibility method took over an hour to run. However, the LB method is more finicky with choice of constants. It is able to simulate higher Reynolds solutions but at the cost that it should use lower velocities and it was less accurate when compared to literature.